Received: 13 July 2023 | Revised: 2 October 2023 | Accepted: 6 October 2023

DOI: 10.1111/cts.13668

SYSTEMATIC REVIEW

Predictability of human exposure by human-CYP3A4-transgenic mouse models: A meta-analysis

David Damoiseaux[1] | **Alfred H. Schinkel**[2] | **Jos H. Beijnen**[1,3] | **Alwin D. R. Huitema**[1,4,5] | **Thomas P. C. Dorlo**[1,6]

[1]Department of Pharmacy & Pharmacology, The Netherlands Cancer Institute, Amsterdam, The Netherlands

[2]Division of Pharmacology, The Netherlands Cancer Institute, Amsterdam, The Netherlands

[3]Utrecht Institute of Pharmaceutical Sciences, Utrecht University, Utrecht, The Netherlands

[4]Department of Pharmacology, Princess Máxima Center for Pediatric Oncology, Utrecht, The Netherlands

[5]Department of Clinical Pharmacy, University Medical Center Utrecht, Utrecht University, Utrecht, The Netherlands

[6]Department of Pharmacy, Uppsala University, Uppsala, Sweden

Correspondence
David Damoiseaux, Plesmanlaan 121, 1066 CX, Amsterdam, The Netherlands.
Email: d.damoiseaux@nki.nl

Abstract

First-in-human dose predictions are primarily based on no-observed-adverse-effect levels in animal studies. Predictions from these animal models are only as effective as their ability to predict human results. To narrow the gap between human and animals, researchers have, among other things, focused on the replacement of animal cytochrome P450 (CYP) enzymes with their human counterparts (called humanization), especially in mice. Whereas research in humanized mice is extensive, the emphasis has been particularly on qualitative rather than quantitative predictions. Because the CYP3A4 enzyme is most involved in the metabolism of clinically used drugs, most benefit was expected from CYP3A4 models. There are several applications of these mouse models regarding in vivo CYP3A4 functionality, one of which might be their capacity to help improve first-in-human (FIH) dose predictions for CYP3A4-metabolized drugs. To evaluate whether human-CYP3A4-transgenic mouse models are better predictors of human exposure compared to the wild-type mouse model, we performed a meta-analysis comparing both mouse models in their ability to accurately predict human exposure of small-molecule drugs metabolized by CYP3A4. Results showed that, in general, the human-CYP3A4-transgenic mouse model had similar accuracy in the prediction of human exposure compared to the wild-type mouse model, suggesting that there is limited added value in humanization of the mouse Cyp3a enzymes if the primary aim is to acquire more accurate FIH dose predictions. Despite the results of this meta-analysis, corrections for interspecies differences through extension of human-CYP3A4-transgenic mouse models with pharmacokinetic modeling approaches seems a promising contribution to more accurate quantitative predictions of human pharmacokinetics.

Study Highlights

WHAT IS THE CURRENT KNOWLEDGE ON THE TOPIC?

Whereas research in humanized mice is extensive, the emphasis has been particularly on qualitative rather than quantitative predictions.

WHAT QUESTION DID THIS STUDY ADDRESS?

Are human-CYP3A4-transgenic mouse models better predictors of human exposure compared to the wild-type mouse model for small-molecule drugs metabolized by CYP3A4?

WHAT DOES THIS STUDY ADD TO OUR KNOWLEDGE?

In general, the human-CYP3A4-transgenic mouse model had similar accuracy in the prediction of human exposure compared to the wild-type mouse model, suggesting that there is limited added value in humanization of the mouse Cyp3a enzymes if the primary aim is to acquire more accurate first-in-human (FIH) dose predictions.

HOW MIGHT THIS CHANGE CLINICAL PHARMACOLOGY OR TRANSLATIONAL SCIENCE?

Humanization of CYP3A enzymes alone is not enough to account for the misspecifications in prediction of human exposure in the context of FIH dosing. Interspecies differences consist of an interplay of many different processes that are vastly more complex. Modern data analysis approaches might help to exploit benefits of human-CYP3A4-transgenic mouse models.

INTRODUCTION

To ensure the safety of participants of first-in-human (FIH) clinical trials of new molecular entities, regulatory guidelines by both the US Food and Drug Administration and European Medicines Agency describe how to derive maximum recommended starting doses.[1-3] The aim is to predict a starting dose close to the therapeutic range, especially for anticancer drugs, in order to acquire phase I objectives (e.g., assessment of the pharmacodynamic and pharmacokinetic [PK] profile and drug tolerability) within a reasonable time, limiting the number of participants treated at subtherapeutic doses while minimizing toxicity at the initial dose. Predictions of the human PKs and pharmacodynamics of a drug are made based on in vitro assays and in vivo animal models prior to exposing humans. The recommended process involves determining the no-observed-adverse-effect levels (NOAELs) in different animal species and converting the NOAEL of the most sensitive species to the human equivalent dose using allometric scaling.[1] For anticancer drugs, the severely toxic dose in 10% of animals is commonly used.[4] Nevertheless, to predict human exposure and toxicity, animal models are only as effective as their ability to predict human results. Hence, the World Health Organization recommends a factor 10 safety margin over the NOAELs to allow for interspecies differences. This factor of 10 is constituted of the subfactors 2.5 and 4.0 for toxicodynamics and toxicokinetics, respectively.[5]

In the late 1980s, researchers acquired the skills to genetically modify animal models by knocking out certain animal genes and replacing them with their human counterparts to better predict the human PKs, a process called humanization. In the field of PKs, the often-observed inconsistency of metabolizing enzymes between species is a common target for humanization, especially in mice.[6] One main purpose for these models was to recognize risks and opportunities for in vivo human drug–drug and drug-food interactions in in vivo mouse settings in a qualitative way. For instance, the human cytochrome P450 (CYP)3A enzymes deviate from the Cyp3as of mice. Mice express eight full-length mouse Cyp3as and humans four CYP3As (CYP3A4, -5, -7, and -43). Despite differences, human CYP3A and mouse Cyp3a have broadly overlapping substrate specificity and tissue expression. Therefore, the biological function of all wild-type mouse Cyp3as combined likely corresponds to the combined function of all human CYP3As.[7] However, because of intrinsic biological differences between these species (e.g., preferred diet), these functionalities are not necessarily identical. Therefore, the wild-type model may not be the most appropriate model to investigate the PKs of drugs for which clearance is highly dependent on CYP3A4-mediated metabolism. For instance, reliably studying drug–drug interactions would be practically impossible because compounds responsible for human CYP3A4 inhibition are not necessarily inhibitors for the mouse Cyp3as (and vice versa).

Because CYP3A4 is the enzyme most frequently involved in metabolism of many clinically used drugs, and often affected by inter- and intra-individual differences in expression and activity,[8] multiple research groups developed humanized CYP3A4 mouse models to investigate the metabolism of CYP3A4. Although human-CYP3A4-transgenic mouse models have mainly been studied for the qualitative translational assessment

of effects of the CYP3A4 enzyme in humans, few studies have focused on the quantitative predictability of the human-CYP3A4-transgenic mouse models over that of the wild-type mouse model. Better quantitative predictions of human exposure could potentially help inform the FIH dose that still requires high margins of safety due to inaccuracy of animal models.[5] We here performed a meta-analysis of the literature in which human-CYP3A4-transgenic mouse models were used to assess the PKs of small molecule drugs. Our aim with this meta-analysis is to evaluate whether the human-CYP3A4-transgenic mouse models provide a better prediction of human exposure than the wild-type mouse models.

METHODS

A literature search for publications presenting quantitative PK information after administration of a small-molecule drug in a human-CYP3A4-transgenic animal model was last performed on the February 6, 2023, using PubMed. The meta-analysis was performed according to the Preferred Reporting Items for Systematic Reviews and Meta-Analyses guidelines, except that screening and reporting was performed by only one reviewer.[9] The full PubMed search and inclusion and exclusion criteria are presented in Figure 1. PubMed was searched using the search term ((cytochrome P450 AND 3a OR 3a4) OR cyp3a4) AND (transgenic OR humanized) AND (pharmacokinetics OR exposure OR AUC OR C_{max} OR (peak concentration)). Exclusion criteria were the absence of useful plasma PK data, CYP3A5/7, chimeric liver transplant mice, reviews, absence of human PKs for drug, last measurable concentration (C_{last}) higher than 1/10th of the maximum plasma concentration (C_{max}), and no possibility for extrapolation until infinity and no or unknown dose proportionality. Extraction of the area under the concentration-time curve extrapolated to infinity (AUC_{0-inf}) from the publication was performed. Either the C_{last} was at least 1/10th of the C_{max} or at least two observed concentrations after the C_{max} were available to calculate the elimination constant (k_e) and extrapolate the AUC_{0-inf} by dividing the C_{last} by the k_e (with the assumption that the studied drug had a single terminal elimination rate constant). Data from concentration-time curves were extracted by means of PlotDigitizer[10] and AUC_{0-inf} calculated using the linear trapezoidal rule with extrapolation. Subsequently, the dose administered in mice was allometrically scaled to a human equivalent dose:

$$\text{Dose scaling factor} = \frac{BW_{human}}{BW_{mouse}}^{\text{exponent}} \quad (1)$$

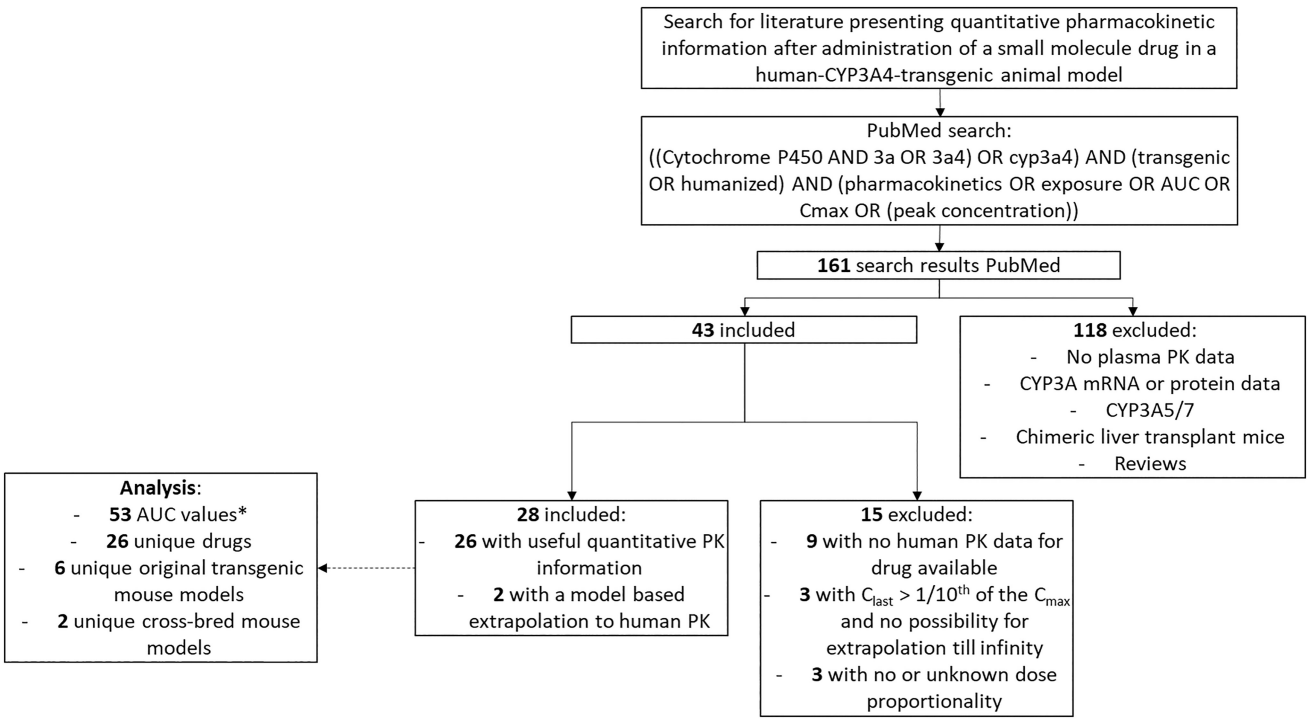

FIGURE 1 Flow diagram of literature search and article selection. *For 20 of the 53 AUC values, the C_{last} are unknown (all AUC_{0-24h}), however, after 24 h, most drugs in mice reach a concentration smaller than 1/10th of the C_{max} and therefore the study was assumed to fulfill the criteria and the AUC values were not excluded (no wild-type mice PK was evaluated in these experiments). AUC, area under the plasma concentration-time curve; C_{last}, last observed concentrations; C_{max}, peak concentrations; PK, pharmacokinetic.

Where BW_{human} and BW_{mouse} represent the bodyweight of an average human and mouse, which were assumed to be 70 and 0.03 kg, respectively. The exponent represents the allometric scaling exponent of either 0.67 or 0.75. An exponent of 0.67 yields a function between BW and clearance that is similar to a linear function between body surface area and clearance. The exponent of 0.75 is used to describe interspecies differences in basal metabolic rate.[11,12] Because they are generally both used, we evaluated both. The AUC_{0-inf} corresponding to the human equivalent dose was extracted from literature. If no data regarding the AUC_{0-inf} were available for the human equivalent dose, the closest available dose with information regarding AUC_{0-inf} was extracted (the fold difference between the scaled and closest available dose ranged from 0.09 to 108; Table S1). The extracted AUC_{0-inf} and dose in this case were linearly scaled to the human equivalent dose under the assumption that the PKs of the drug of interest were dose proportional. Last, all AUC_{0-inf} units were converted to ng/mL h and mouse AUC_{0-inf} were compared to human AUC_{0-inf} for the accuracy in the prediction of human exposure. A schematic overview of the methods is presented in Figure 2.

Comparison of the deviations of mouse AUC_{0-inf} from human AUC_{0-inf} for multiple drugs results in higher absolute errors for drugs that have higher AUC_{0-inf} despite a low relative error, which is more informative here. To give equal weights to the predictability of the mouse model for the human exposure for each compound we calculated the fold differences from the human AUC_{0-inf}. In order to calculate mean errors of the fold differences, normalization across fold differences smaller and larger than one are required. Fold differences were normalized using Equation 2:

$$\text{Normalized fold difference} = 10^{|\log_{10}\text{fold difference}|}, \quad (2)$$

Subsequently, normalized fold differences were used to calculate the mean absolute error (MAE) and the root mean squared error (RMSE).

$$\text{MAE} = \frac{1}{n}\sum_{i=1}^{n}|y_i - \hat{y}_i|, \quad (3)$$

$$\text{RMSE} = \sqrt{\sum_{i=1}^{n}\frac{(\hat{y}_i - y_i)^2}{n}}, \quad (4)$$

Where y_i represents the observation and $\hat{y}_i$ the prediction.

The mouse model resulting in lower median errors and the least dispersion was considered a better predictor of the human exposure. Processing of the data and graphical and statistical diagnostics were performed with R (version 4.2.1).

RESULTS

The literature search resulted in 161 publications. Of these, 28 met our inclusion criteria and were used for the analysis. A flow diagram of the inclusion and exclusion

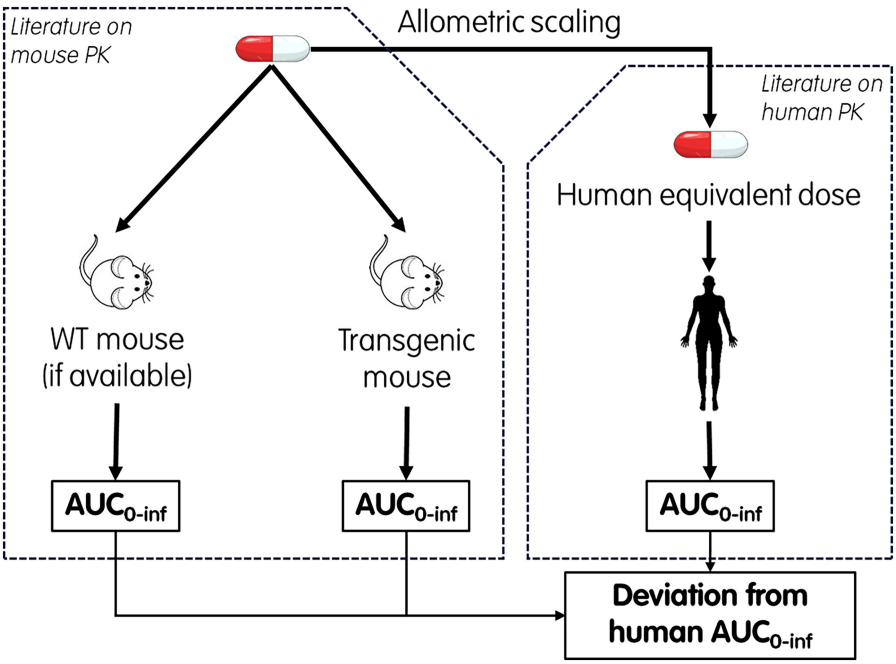

FIGURE 2 Schematic presentation of the methods. AUC_{0-inf}, area under the plasma concentration-time curve until infinity; PK, pharmacokinetic; WT, wild-type.

is presented in Figure 1. After exclusion, only studies in mice were described in the remaining publications. We identified eight publications that described the development of human-CYP3A4-transgenic mouse models (original transgenic mouse models; Table 1). Two publications (Abe et al. and Cheung et al.[13,14]) were not used to evaluate the PKs of any drug (also not in other publications) and three publications (Hasegawa et al., Kazuki et al. and Ma et al.[15-17]) describing the original transgenic mouse models did not present drug PKs itself or did not meet the inclusion criteria (other publications did evaluate the PKs of drugs using these models). Furthermore, two crossbred models have been developed by Uehara et al. and Scheer et al. by crossbreeding previously developed human-CYP3A4-transgenic mouse models.[18,19] Within the 28 included publications, two publications (Damoiseaux et al. and Zhang et al.[20,21]) used modeling approaches to extrapolate human-CYP3A4-transgenic mouse model PKs to human PKs and were included for discussion. Fifty-three AUC_{0-inf} were derived from the other 26 publications (Tables 2 and S1) containing 26 unique drugs administered in human-CYP3A4-transgenic mouse models developed by eight different mouse model developers (of which two crossbred). From 17 of the 26 publications, also the AUC_{0-inf} in wild-type mice could be derived (for 19 of the 53 AUC_{0-inf} in human-CYP3A4-transgenic mice). Additionally, Table 3 presents human drug exposures reported in the literature after administration of a single dose of the drugs that were also evaluated in the mouse models, as well as to what extent they are metabolized by CYP3A4.

Results of the analysis are presented in Figures 3–5 and Tables S1 and S2. Figure 3 presents all 53 human-CYP3A4-transgenic mouse AUC_{0-inf} and 19 wild-type mouse AUC_{0-inf} in relation to the human AUC_{0-inf} after administration of an equivalent dose as absolute values and fold differences. Extrapolation with the exponent 0.67 resulted in a symmetric distribution of the fold differences in AUC_{0-inf} between human and both human-CYP3A4-transgenic and wild-type mice around 1.13 and 1.02-fold, respectively (where 1-fold is an exact prediction of the AUC_{0-inf}; Figure 4b). Extrapolation with the exponent 0.75 resulted in a symmetric distribution around a median of 0.61 and 0.55-fold for human-CYP3A4-transgenic and wild-type mice, respectively. This suggests that using the allometric scaling exponent 0.67 results in more accurate predictions of the human equivalent dose than the exponent 0.75.

To perform a comparison between human-CYP3A4-transgenic and wild-type mice for the predictability of the human equivalent dose, a selection was made of publications, which presented AUC_{0-inf} for both human-CYP3A4-transgenic and wild-type mice (19 AUC_{0-inf} each;

TABLE 1 Publications describing human-CYP3A4-transgenic mouse models.

Model	Human P450 transgene structure	Promoter	Mouse gene knockout for humanization	References
CYP3A4-transgenic	Gene (BAC)	Authentic	None	Granvil et al.[31]
CYP3A4-transgenic	cDNA	Human ApoE promoter	None	van Herwaarden et al.[32]
CYP3A4-humanized	cDNA	Human ApoE promoter or mouse villin promoter	Cyp3a-null	van Herwaarden et al.[7]
CYP3A4/3A7-transgenic	Gene (BAC)	Authentic	None	Cheung et al.[14]
CYP3A4/3A7-transgenic	Gene (BAC)	Authentic (PXR humanized)	None	Ma et al.[17]
CYP3A4/3A7-humanized	Gene (modified BAC)	Authentic (PXR and CAR humanized)	Cyp3a-null (except for Cyp3a13)	Hasegawa et al.[15]
CYP3A4/3A5*3/3A7/3A43-humanized	Gene (HAC)	Authentic (CYP3A5 not expressed)	Cyp3a-null	Kazuki et al.[16]
CYP3A4/3A5*1/3A7/3A43-humanized	Gene (modified HAC)	Authentic (CYP3A5 expressed)	Cyp3a-null	Abe et al.[13]

Models developed by crossbreeding of human-CYP3A4-transgenic mouse models were not included. Information originates from Table 1, Bissig et al.[6]Abbreviations: ApoE, Apolipoprotein E; BAC, bacterial artificial chromosome; CAR, constitutive androstane receptor; HAC, human artificial chromosome; PXR, Pregnane X receptor.

TABLE 2 Summary of all included publications presenting quantitative pharmacokinetic information after administration of a small-molecule drug in a human-CYP3A4-transgenic mouse model.

References	Category[a]	Evaluated drugs	Mice model developer	Crossbred mice model developer	Wild-type mice PK available?	Administered Dose (mg/kg) (oral unless indicated otherwise)
Choo, E. F., et al.[33]	Application	Cobimetinib	Hasegawa et al.; Van Herwaarden et al. 2007	NA	Yes	5
Damoiseaux, D., et al.[34]	Application	Lorlatinib	Van Herwaarden et al. 2007	NA	Yes	10
Granvil, C. P., et al.[31]	Original	Midazolam	Granvil et al.	NA	Yes	2.5 (oral); 0.25 (i.v.)
Hasegawa, M., et al.[35]	Application	Triazolam	Hasegawa et al.	NA	No	5
Henderson, C. J., et al.[36]	Application	Caffeine, debrisoquine, midazolam, tolbutamide, dabrafenib, sulfaphenazole, S-Acenocoumarol, Hyperforin	Hasegawa et al.	Scheer et al.	No	10 dabrafenib; 3 midazolam; 25 osimertinib
Kim, S., et al.[37]	Application	Triazolam	Ma et al.	NA	No	4
Kobayashi, K., et al.[38]	Application	Triazolam	Kazuki et al.	NA	No	1
Li, W., et al.[39]	Application	Lorlatinib	Van Herwaarden et al. 2007	NA	Yes	10
Li, W., et al.[40]	Application	Lorlatinib	Van Herwaarden et al. 2007	NA	Yes	10
Li, W., et al.[41]	Application	Fisogatinib	Van Herwaarden et al. 2007	NA	Yes	10
Li, W., et al.[42]	Application	Galunisertib	Van Herwaarden et al. 2007	NA	Yes	20
Ly, J. Q., et al.[43]	Application	Alprazolam, bosutinib, crizotinib, dasatinib, gefitinib, ibrutinib, regorafenib, sorafenib, triazolam, vandetanib	Hasegawa et al.; Van Herwaarden et al. 2007	NA	No	5

Reported AUC for transgenic mice	Reported AUC for transgenic mice wild-type	AUC time interval	C_{last} lower than 1/10th of C_{max}?	AUC_{0-inf} for transgenic mice (ng/mL h)	AUC_{0-inf} for wild-type mice (ng/mL h)
0.701 ± 0.087 μM h (van Herwaarden); 3.95 ± 0.58 μM h (Hasegawa)	1.38 ± 0.25 μM h	0–24 h	Yes	372.4 (van Herwaarden); 2098.6 (Hasegawa)	733.2
7.8 ± 1.3 μg/mL h; 9.2 ± 1.5 μg/mL h	13.3 ± 2.2 μg/mL h; 17.2 ± 3.0 μg/mL h	0–8 h; 0–inf	Yes	9200.0	17200.0
8330 nmol/L min (oral); 8390 nmol/L min (i.v.)	13,800 nmol/L min (oral); 6530 nmol/L min (i.v.)	0–inf	Yes	45.0 (oral) 45.3 (i.v.)	74.5 (oral) 35.3 (i.v.)
1210 ± 110 ng/mL h	NA	0–inf	Yes	1210.0	NA
21,925 ± 1687 ng/mL h dabrafenib; 462 ± 70 ng/mL h midazolam; 3753 ± 614 ng/mL h osimertinib (no PK for other drugs)	NA	0–25 h (dabrafenib); 0–inf (midazolam); 0–32 h (osimertinib)	Yes	21925.0 (dabrafenib) 462.0 (midazolam) 3753.0 (osimertinib)	NA
1583 nM h	NA	0–6 h	No (1/8th C_{max})	569.7	NA
1050 ± 242 nM h; 448 ± 157 nM h	NA	0–inf	Yes	153.7	NA
11,701 ± 1274 ng/mL h	7585 ± 533 ng/mL h	0–8 h	No (half C_{max})	12557.3	10553.2
5792 ± 871 ng/mL h	10,542 ± 1067 ng/mL h	0–8 h	No (half C_{max})	7972.0	16699.1
4284 ± 600 ng/mL h	5072 ± 823 ng/mL h	0–4 h	No (1/5th C_{max})	5956.8	4753.4
4095 ± 1262 ng/mL h	2706 ± 640 ng/mL h	0–1 h	Yes	4095.0	2706.0
8.07 ± 3.47 Alprazolam, 0.41 ± 0.21 bosutinib, 0.616 ± 0.128 crizotinib, 0.105 ± 0.035 dasatinib, 0.89 ± 0.06 gefitinib, 0.174 ± 0.058 ibrutinib, 4.9 ± 1.53 regorafenib, 8.44 ± 3.22 sorafenib, 0.22 ± 0.046 triazolam, 10.2 ± 1.92 vandetinib (μM h, van Herwaarden) --- 3.1 ± 0.23 Alprazolam, 1.84 ± 0.35 bosutinib, 0.213 ± 0.08 crizotinib, 0.119 ± 0.08 dasatinib, 1.68 ± 0.39 gefitinib, 0.567 ± 0.105 ibrutinib, 2.67 ± 0.4 regorafenib, 8.02 ± 1.15 sorafenib, 1.15 ± 0.21 triazolam, 6.88 ± 1.55 vandetinib (μM h, Hasegawa)	NA	0–24 h	Unknown	2492.0 alprazolam, 217.5 bosutinib, 279.2 crizotinib, 53.7 dasatinib, 397.7 gefitinib, 74.9 ibrutinib, 2365.7 regorafenib, 3922.9 sorafenib, 75.5 triazolam, 4889.9 vandetinib (van Herwaarden) --- 957.3 alprazolam, 975.9 bosutinib, 94.6 crizotinib, 58.6 dasatinib, 750.8 gefitinib, 251.1 ibrutinib, 1289.1 regorafenib, 3727.7 sorafenib, 394.7 triazolam, 3298.3 vandetinib (Hasegawa)	NA

TABLE 2 (Contiuned)

References	Category[a]	Evaluated drugs	Mice model developer	Crossbred mice model developer	Wild-type mice PK available?	Administered Dose (mg/kg) (oral unless indicated otherwise)
MacLeod, A. K., et al.[44]	Application	Vemurafenib	Hasegawa et al.	Scheer et al.	No	50 and 100
MacLeod, A. K., et al.[45]	Application	Osimertinib	Hasegawa et al.	Scheer et al.	Yes	25
Martínez-Chávez, A., et al.[46]	Application	Ribociclib	Van Herwaarden et al. 2007	NA	Yes	20
Martínez-Chávez, A., et al.[47]	Application	Abemaciclib	Van Herwaarden et al. 2007	NA	Yes	10
Miura, T., et al.[48]	Application	S-warfarin, Diclofenac	Hasegawa et al.	NA	No	0.5 warfarin; 10 diclofenac (both i.v.)
ML, F. M., et al.[49]	Application	Niraparib	Van Herwaarden et al. 2007	NA	Yes	50
Scheer, N., et al.[19]	Crossbred	Midazolam	Hasegawa et al.	Scheer et al.	No	5
Uehara, S., et al.[18]	Application	caffeine, warfarin, omeprazole, metoprolol, midazolam	Hasegawa et al.	Uehara et al.	No	10
van Herwaarden, A. E., et al.[32]	Original	Midazolam, Cyclosporin A	Van Herwaarden et al. 2005	NA	Yes	30 midazolam; 20 cyclosporin A (both i.v.)
van Herwaarden, A. E., et al.[7]	Original	Docetaxel	Van Herwaarden et al. 2007	NA	Yes	10 (i.v.)
van Hoppe, S., et al.[22]	Application	Ibrutinib	Van Herwaarden et al. 2007	NA	Yes	10
van Waterschoot, R. A., et al.[50]	Application	Triazolam	Van Herwaarden et al. 2007	NA	Yes	0.5
Wang, J., et al.[51]	Application	Tivozanib	Van Herwaarden et al. 2007	NA	Yes	1
Yamazaki, H., et al.[52]	Application	Midazolam	Hasegawa et al.	NA	Yes	10 (i.v.)

Abbreviations: AUC_{0-inf}, from zero to infinite hour; AUC, area under the plasma concentration-time curve; C_{last}, last observed concentrations; C_{max}, peak concentrations; NA, not applicable; PK, pharmacokinetics.

[a]The column category consists of: original publications that describe the development of a human-CYP3A4-transgenic mouse model; crossbred, publications that describe the crossbreeding of a human-CYP3A4-transgenic mouse model; application, publications that describe pharmacokinetic experiments using a human-CYP3A4-transgenic mouse model.

Figure 4). The selection resulted in a narrower interval between the first and third quartiles in the AUC_{0-inf} distributions for human-CYP3A4-transgenic compared to wild-type mice (Figure 4b), suggesting that human-CYP3A4-transgenic mice are more accurate predictors of the human exposure than wild-type mice for most drugs. However, allometric scaling with the exponent 0.67 resulted in a higher RMSE for human-CYP3A4-transgenic than wild-type mice, 6.82 versus 4.96-fold (normalized), respectively (Figure 5). For allometric scaling with the exponent 0.75, the RSME were 5.44 versus 5.10-fold (normalized), respectively. The MAE was slightly lower for the human-CYP3A4-transgenic compared to wild-type mice, 3.05 versus 3.08-fold (normalized) for the exponent 0.67 and 3.06 versus 3.19-fold

Reported AUC for transgenic mice	Reported AUC for transgenic mice wild-type	AUC time interval	C_{last} lower than 1/10th of C_{max}?	AUC_{0-inf} for transgenic mice (ng/mL h)	AUC_{0-inf} for wild-type mice (ng/mL h)
294 μg/mL h (50 mg/kg), huCYP3A4/3A7; 432 μg/mL h (50 mg/kg), 559 μg/mL h (100 mg/kg), huPXR/huCAR/huCYP3A4/3A7	NA	0–inf	Yes	294,000 (50 mg/kg) huCYP3A4/3A7; 432,000 (50 mg/kg), 559,000 (100 mg/kg), huPXR/huCAR/huCYP3A4/3A7	NA
1144 ± 363 ng/mL h	998 ± 419 ng/mL h	0–24 h	Yes	1144.0	998.0
1834 ± 490 ng/mL h	5901 ± 1760 ng/mL h	0–8 h	No (1/3rd C_{max})	2173.1	7443.9
3200 ± 791 nM h	7808 ± 1837 nM h	0–24 h	Yes	1622.4	3958.7
8.3 ± 2.4 nmol/mL h (S-warfarin); 41.1 ± 7.5 nmol/mL h (diclofenac)	NA	0–inf	Yes	12165.6 (diclofenac) (S-warfarin excluded)	NA
56,463 ± 10,785 ng/mL h	25,919 ± 6309 ng/mL h	0–24 h	Yes	18068.2	8294.1
125 μg/mL min	NA	0–24 h	Yes	2083.3	NA
13 ± 3 caffeine; 58 ± 11 warfarin; 0.022 ± 0.010 omeprazole; 0.038 ± 0.002 metoprolol; 0.098 ± 0.017 midazolam (μg/mL h)	NA	0–inf	Yes	20.0 (omeprazole) 100.0 (midazolam) (caffeine, warfarin and metoprolol excluded)	NA
5.45 μg/mL h (midazolam); 24.3 μg/mL h (cyclosporin A)	11.7 μg/mL h (midazolam); 35.8 μg/mL h (cyclosporin A)	0–3 h (midazolam); 0–8 h (cyclosporin A)	Yes (midazolam); No 1/7th C_{max} (cyclosporin A)	5450.0 (midazolam) 31800.0 (cyclosporine A)	11700.0 (midazolam) 48020.0 (cyclosporine A)
976.9 ng/mL h	777 ng/mL h	0–8 h	Yes	976.9	777.0
832 ± 521 ng/mL h	431 ± 96.6 ng/mL h	0–8 h	Yes	832.0	431.0
130 ± 19 μg/L h	194 ± 23 μg/L h	0–5.3 h	No (1/3rd C_{max})	176.2	NA
6227 ± 936 ng/mL h	4557 ± 683 ng/mL h	0–24 h	Yes	6227.0	4557.0
759 ± 431 μM min	536 ± 46 μM min	0–inf	Yes	4121.1	2910.3

(normalized) for the exponent 0.75, respectively. Removal of the extreme outlier ibrutinib resulted in results in favor of the human-CYP3A4-transgenic mice. Allometric scaling with the exponent 0.67 resulted in a lower RMSE for human-CYP3A4-transgenic than wild-type mice, 2.88 versus 3.96-fold (normalized), respectively (Figure 5). For allometric scaling with the exponent 0.75, the RSME were 4.49 versus 4.98-fold (normalized), respectively. The MAE was also lower for the human-CYP3A4-transgenic compared to wild-type mice, 1.72 versus 2.50-fold (normalized) for the exponent 0.67 and 2.44 versus 2.99-fold (normalized) for the exponent 0.75, respectively.

Large variability was observed between experiments with the same compound (ibrutinib and triazolam) and

TABLE 3 Reported human drug exposure after administration of a single dose.

Drug (oral unless indicated otherwise)	CYP3A4 metabolized drug?	Degree of CYP3A4 mediated metabolism of drug	Drug class
Abemaciclib	Yes	Extensively	L01EF03 (Antineoplastic agents)
Alprazolam	Yes	Primarily	N05BA12 (Psycholeptics)
Bosutinib	Yes	Primarily	L01EA04 (Antineoplastic agents)
Cobimetinib	Yes	Primarily	L01EE02 (Antineoplastic agents)
Crizotinib	Yes	Primarily	L01ED01 (Antineoplastic agents)
Cyclosporin A (i.v.)	Yes	Extensively	L04AD01 (Immunosuppressants)
Dabrafenib	Yes	Primarily	L01EC02 (Antineoplastic agents)
Dasatinib	Yes	Primarily	L01EA02 (Antineoplastic agents)
Diclofenac (i.v.)	No	NA	M01AB55 (Anti-inflammatory and antirheumatic products)
Docetaxel (i.v.)	Yes	Primarily	L01CD02 (Antineoplastic agents)
Fisogatinib	Yes	Unknown	Unknown
Galunisertib	Unlikely	Unknown	Unknown
Gefitinib	Yes	Partly	L01XX31 (Antineoplastic agents)
Ibrutinib	Yes	Primarily	L01EL01 (Antineoplastic agents)
Lorlatinib	Yes	Primarily	L01ED05 (Antineoplastic agents)
Midazolam	Yes	Extensively	N05CD08 (Psycholeptics)
Midazolam (i.v.)	Yes	Extensively	N05CD08 (Psycholeptics)
Niraparib	Yes	Extensively	L01XX54 (Antineoplastic agents)
Omeprazole	Yes	To lesser extent (mainly CYP2C19)	A02BC01 (Acid related disorders)
Osimertinib	Yes	Primarily	L01EB04 (Antineoplastic agents)
Regorafenib	Yes	Primarily	L01EX05 (Antineoplastic agents)
Ribociclib	Yes	Primarily	L01EF02 (Antineoplastic agents)
Sorafenib	Yes	Primarily	L01EX02 (Antineoplastic agents)
Tivozanib	Yes	Partly	L01EK03 (Antineoplastic agents)
Triazolam	Yes	Primarily	N05CD05 (Psycholeptics)
Vandetanib	Yes	Partly	L01EX04 (Antineoplastic agents)
Vemurafenib	Yes	To lesser extend	L01XE15 (Antineoplastic agents)

Abbreviations: 0–inf, from zero to infinite hour; AUC, area under the plasma concentration–time curve; C_{last}, last observed concentrations; C_{max}, peak concentrations; i.v., intravenous; NA, not applicable; PK, pharmacokinetics.

[a]Data extracted from concentrations–time curves by means of PlotDigitizer[10] and AUC_{0-inf} calculated using the trapezoidal rule.

Reference human PK data	Reported AUC for human	AUC time interval	C_{last} lower than 1/10th of C_{max}?	Calculated AUC_{0-inf}
Patnaik A, et al. (2016)[53]	1270 ng/mL h (50 mg); 1880 ng/mL h (100 mg); 4010 ng/mL h (150 mg); 5220 ng/mL h (200 mg)	0–inf	Yes	NA
Friedman H, et al. (1991)[54]	305 ng/mL h (1 mg)	0–50 h	No, 1/9th C_{max}	316.6 ng/mL h
Abbas R, et al. (2011)[55]	323 ng/mL h (100 mg)	0–inf	Yes	NA
Rosen LS, et al. (2016)[56]	1556 ng/mL h (40 mg)[a]; 3112 ng/mL h (60 mg)[a]	0–24 h[a]	Yes	NA
Xu H, et al. (2015)[57]	1260 ng/mL h (150 mg); 2192 ng/mL h (250 mg)	0–inf	Yes	NA
Gupta SK, et al. (1990)[58]	8799 ng/mL h (4 mg/kg, 64 kg)	0–24 h	Yes	NA
Ouellet D, et al. (2013)[59]	9858 ng/mL h (150 mg)	0–inf	Yes	NA
Christopher LJ, et al. (2008)[60]	1151 ng/mL h (180 mg)	0–24 h	Yes	NA
Leuratti C, et al. (2019)[61]	5384 ± 1020 ng/mL h (75 mg; i.v. bolus)	0–inf	Yes	NA
Baker SD, et al. (2006)[62]	3.41 μg/mL h (75 mg/m^2; 1 h infusion)	0–inf	Yes	NA
Kim RD, et al. (2019)[63]	24,420 ng/mL h (140 mg)[a]; 128,564 ng/mL h (600 mg)[a]	0–24 h[a]	Yes	NA
Ding X, et al. (2015)[64]	3670 μg/L h (150 mg, solution)	0–inf	Yes	NA
Ranson M, et al. (2002)[65]	1147 ng/mL h (50 mg)	0–140 h	Yes	NA
Tapaninen T, et al. (2020)[66]	76.5 ng/mL h (140 mg)	0–inf	Yes	NA
Patel M, et al. (2020)[67]	7338 ng/mL h (100 mg)	0–inf	Yes	NA
Stroh M, et al. (2010)[68]	102 ng/mL h (7.5 mg)	0–inf	Yes	NA
Pentikis HS, et al. (2007)[69]	84.76 ng/mL h (2 mg; i.v. bolus)	0–inf	Yes	NA
Moore K, et al. (2018)[70]	29016.1 ng/mL h (300 mg, fasted)	0–inf	Yes	NA
Ochoa D, et al. (2020)[71]	2190.8 ± 2011.5 ng/mL h (40 mg, fasted)	0–inf	Yes	NA
Planchard D, et al. (2016)[72]	2658 nM h (40 mg, 0–72 h); 5102 nM h (80 mg, 0–72 h); 15,480 nM h (160 mg, 0–72 h); 24,610 nM h (160 mg, 0–inf)	0–72 h or 0–inf	Yes	NA
Zhang Q, et al. (2021)[73]	11354.7 ± 3323.9 ng/mL h (40 mg reference drug)	0–inf	Yes	NA
Ji Y, et al. (2020)[74]	10,700 ng/mL h (600 mg)	0–inf	Yes	NA
Lathia C, et al. (2005)[75]	11.04 mg/L h (50 mg)	0–inf	Yes	NA
Cotreau MM, et al. (2015)[76]	2223 ng/mL h (1.5 mg)	0–inf	Yes	NA
Robin DW, et al. (1993)[77]	15.57 ± 1.54 ng/mL h (0.25 mg)	0–inf	Yes	NA
Martin P, et al. (2012)[78]	22,030 ng/mL h (300 mg); 29,460 ng/mL h (400 mg); 61,140 ng/mL h (800 mg); 102,200 ng/mL h (1200 mg)	0–inf	Yes	NA
Ribas A, et al. (2014)[79]	119.0 ± 113.1 μg/mL h (960 mg, fasted)	0–inf	Yes	NA

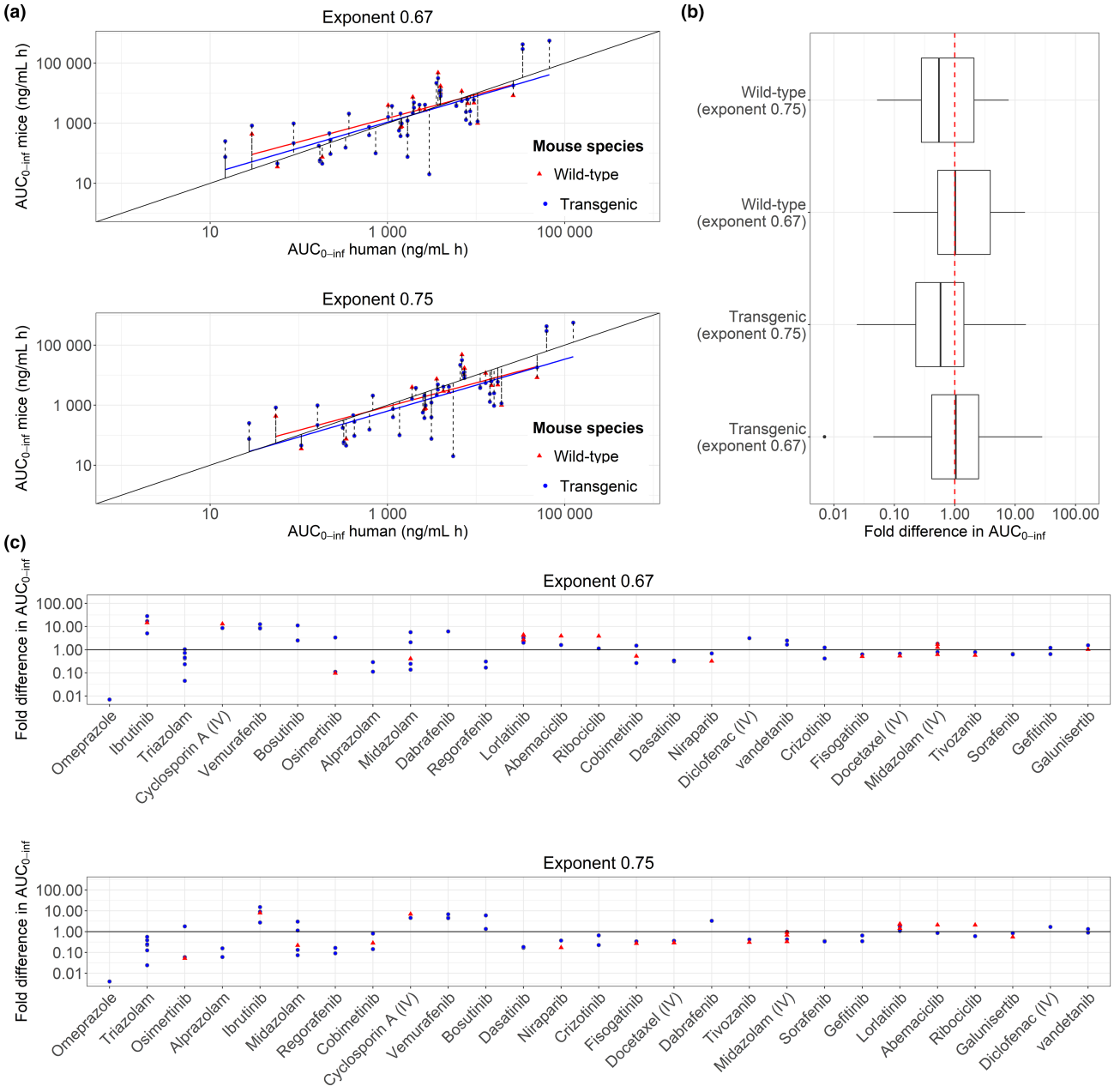

FIGURE 3 (a) The AUC_{0-inf} of human-CYP3A4-transgenic and wild-type mice plotted against the human AUC_{0-inf} after a human equivalent dose, (b) the distribution of the fold differences in AUC_{0-inf} between human and mice, and (c) the fold differences in AUC_{0-inf} between human and mice for each drug. Results from allometric scaling of the mice to human dose with the exponent 0.67 and 0.75 were both presented in all plots. Dotted lines in (a) represent the deviation from the line of unity (an ideal prediction of the human AUC_{0-inf}). Red and blue line represent the trend lines for wild-type and human-CYP3A4-transgenic mice, respectively. All drugs were administered orally unless indicated differently. AUC_{0-inf}, area under the plasma concentration-time curve until infinity.

human-CYP3A4-transgenic mice (Table S1). Finally, between 57% and 79% of the predictions of both human-CYP3A4-transgenic and wild-type mice fell within the toxicokinetic safety margin of four-fold recommended by the World Health Organization to allow for interspecies differences and between 87% and 95% fell within the safety margin of 10-fold for toxicokinetics and toxicodynamics combined, with no clear advantage for either mouse model (Table S2).[5]

DISCUSSION

Human-CYP3A4-transgenic mouse for quantitative predictions in humans

Perhaps contrary to expectations, humanization of the mouse Cyp3a enzymes by means of knock-out and replacement with the human CYP3A4 enzyme in general does not improve the predictions of exposure for

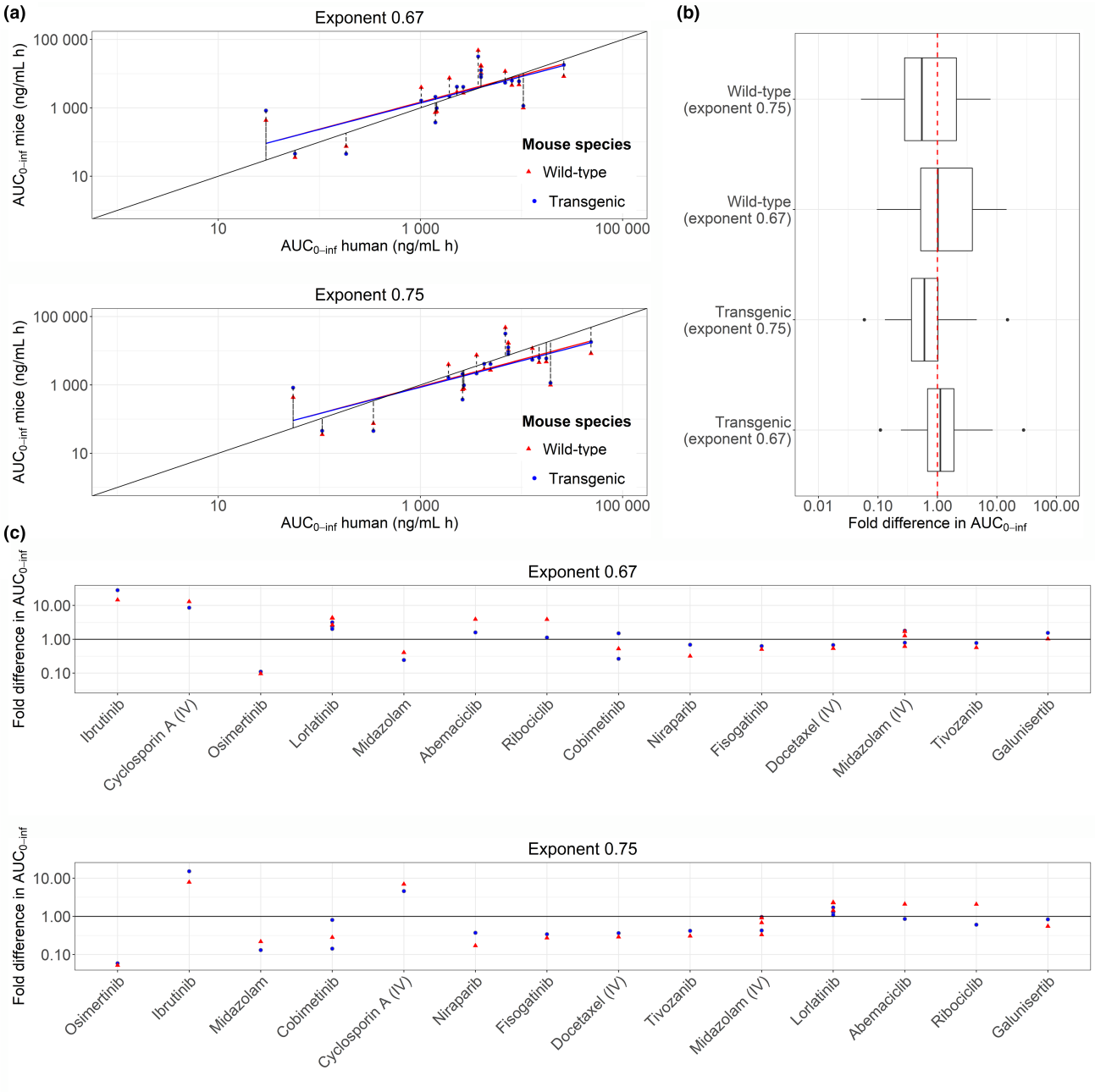

FIGURE 4 A selection of the publications which presented AUC_{0-inf} for both human-CYP3A4-transgenic and wild-type mice (19 AUC_{0-inf} each): (a) the AUC_{0-inf} of human-CYP3A4-transgenic and wild-type mice plotted against the human AUC_{0-inf} after a human equivalent dose, (b) the distribution of the fold differences in AUC_{0-inf} between human and mice, and (c) the fold differences in AUC_{0-inf} between human and mice for each drug. Results from allometric scaling of the mice to human dose with the exponent 0.67 and 0.75 were both presented in all plots. Dotted lines in (a) represent the deviation from the line of unity (an ideal prediction of the human AUC_{0-inf}). Red and blue line represent the trend lines for wild-type and human-CYP3A4-transgenic mice, respectively. All drugs were administered orally unless indicated differently. AUC_{0-inf}, area under the plasma concentration-time curve until infinity.

CYP3A4-metabolized drugs in humans. This result is mainly based on PK experiments in two mouse models developed by Hasegawa et al. and van Herwaarden et al. (Figure S1). Based on the RMSE, the human-CYP3A4-transgenic mouse model performs worse than the wild-type mouse model. This is mainly caused by one extreme outlier, ibrutinib, in predictions of the human-CYP3A4-transgenic mouse model. Nevertheless, there is no obvious reason for excluding this drug because it is mainly metabolized by CYP3A4.[22] On the other hand, the percentage of predictions within four-fold and 10-fold difference from the human exposure are slightly in favor of the human-CYP3A4-transgenic mouse model (Table S2). Everything considered, the

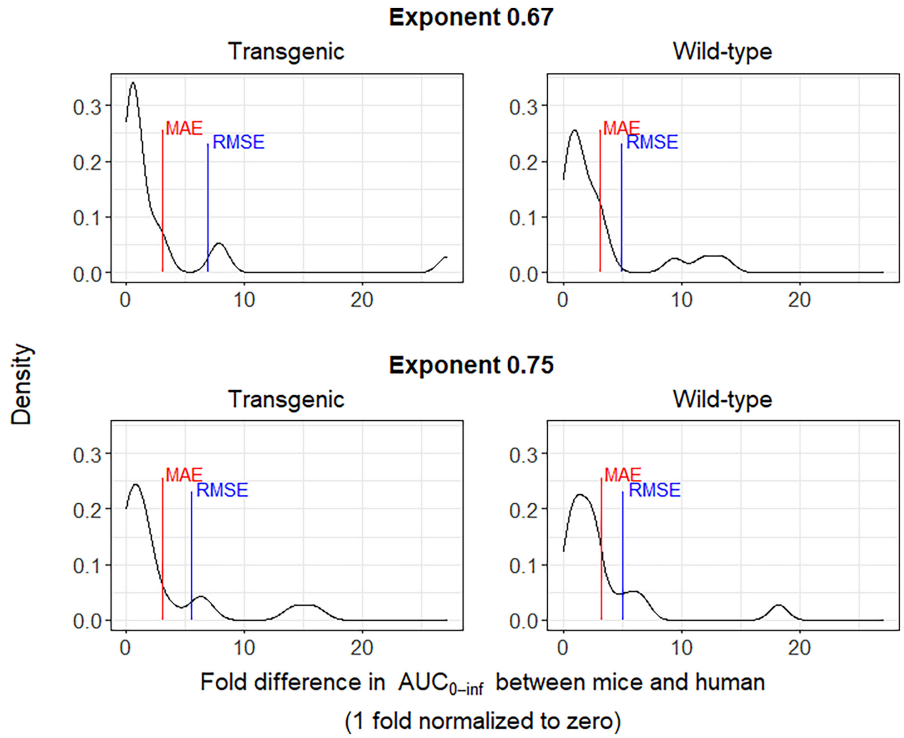

FIGURE 5 Density plots of the fold differences in AUC_{0-inf} between mice and human for the exponents 0.67 and 0.75 for each study. To normalize fold differences to only values higher than one, one was divided by all the fold differences smaller than one. In addition, one was subtracted from all fold differences to normalize a perfect prediction (of 1-fold) to zero. AUC_{0-inf}, area under the plasma concentration-time curve until infinity; MAE, mean absolute error; RMSE, root mean squared error.

small differences in predictability of human exposure suggest that the human-CYP3A4-transgenic mouse model will not markedly contribute to more accurate predictions of exposure following FIH doses in clinical trials by means of allometric scaling.

Difficulties in interspecies extrapolation

The CYP enzymes originate from a gene family that can be found in a wide range of organisms ranging from bacteria, plants, animals to humans, and even viruses. Over time, all species developed different variants of CYP enzymes with part having a common pivotal role, the detoxification of xenobiotics. It has been 75–125 million years ago that mice and humans had a common ancestor. The overlap in absorption, distribution, metabolism, and excretion (ADME) related processes probably stems from exposure to similar xenobiotics over this period, which resulted in similar evolutionary properties. This might explain why the wild-type mice themselves already perform relatively well in the prediction of human exposure. Nevertheless, species have since then adapted to the exposure to partly different xenobiotics, resulting in deviation in detoxifying CYP enzymes to a greater or lesser extent, and the same applies for other ADME-related processes. It is therefore important to elucidate what interspecies differences are responsible for these deviations in order to account for them in advance. Our hypothesis was that humanization of mouse CYP3A enzymes could be an important contributor to the reduction of the error in the predictions of human exposure. However, as it turns out, humanization of CYP3A enzymes alone is not nearly enough to account for the misspecifications in prediction of human exposure in the context of FIH dosing. Distinguishing two species by pinpointing one specific process (like CYP3A-mediated metabolism) proves to be unrealistic. Interspecies differences consist of an interplay of many different processes that are vastly more complex, where the absence of a certain process in a species can be compensated by other processes.[23] Here, we will discuss several examples of other interspecies differences that might contribute to the misspecifications observed in mice to human extrapolation.

First, the absorption of orally administered drugs is highly dependent on the biopharmaceutics classification system (BCS) class of a drug. The permeability and solubility define the class to which a drug is designated. However, the BCS classification in humans does not necessarily apply to mice. Solubility of drugs with a basic pK_a is different in the gastrointestinal tract of mice compared to humans. This is because the normal murine gastric pH is 3–4 and declines to an intestinal pH ~ 5,[24] whereas the

human gastric pH is 1–2.5, and intestinal pH is 6.5–7.5.[25] As a result, absorption profiles differ because a drug can be fully protonated and ionized in the human stomach, whereas only partially in the mouse stomach. In addition, drugs are often administered as a solution by gavage into the stomach in mice, as opposed to solid dosing forms in humans.

Second, variation between experiments with the same drug and animal species is a topic that appears underexposed in the literature. It has been demonstrated that despite strict standardization of experiments, animals can behave differently between different laboratories[26] and it is also been shown that mouse phenotypes can fluctuate, resulting in different results between batches.[27] Consultation with preclinical scientists working with laboratory animals confirmed that deviations of about two-fold in absolute drug concentrations between PK experiments of the same drug and mouse species over time (e.g., 6 months apart), even performed in one facility, is not uncommon. This is less of a concern if groups of animal strains within an experiment are treated equally and within a limited period of time, and only directly compared with each other. This results in minimal variability between groups apart from the investigated difference between the strains. In that context, continuity of absolute values (drug concentrations) over multiple experiments over a prolonged period of time is of lesser concern for answering certain hypotheses. However, for reliable quantitative predictions of the FIH dose, consistency over experiments and especially over time is warranted.

Third, replacing CYP3A enzymes in mice with human CYP3A enzymes does not necessarily imply that the corresponding overall metabolism will be similar. Expression and quantity of the replaced CYP3A enzymes can differ from that in humans, resulting in higher or lower clearance of the drug in the corresponding organ. For instance, van Herwaarden et al. suggests that CYP3A4 expression in the intestines of their transgenic strain is higher in mice compared to humans, which potentially results in lower bioavailability in mice.[7] Probably, there are many more physiological differences between mice and human that can influence drug PKs that still have to be elucidated. An example is a plasma protein expressed by mice, carboxylesterase 1c, which is absent in human plasma resulting in poor translation from mice to humans if the drug PK is influenced by carboxylesterase 1c through metabolism or strong binding.[28] For example, cabazitaxel and everolimus are known to have high binding affinity to this protein resulting in PK differences between human and mouse.[29,30] In short, developing a mouse model that would suit all drugs would require many modifications with still a possibility of missing crucial ADME processes. More importantly, the trade-off must be made as to whether the investments are worth the gains considering the already quite good performance of the wild-type mice in terms of quantitative predictions (at least, for the panel of drugs considered in this analysis).

Other applications for the human-CYP3A4-transgenic mouse model

Despite the results of this meta-analysis, the benefits of human-CYP3A4-transgenic mouse models for quantitative predictions of the human PKs could potentially be further exploited using modern data analysis approaches. More in depth knowledge of PKs in genetically modified animals can be obtained using PK modeling. In addition to finding a difference in exposure, PK modeling can uncover knowledge on the underlying PK processes that are potentially altered by drug metabolizing enzymes. The human-CYP3A4-transgenic mouse model will probably be more representative for the underlying PK processes for human CYP3A4. The human-CYP3A4-transgenic mouse model is therefore likely to be more accurate in the prediction of drug–drug interactions (DDIs) in which this enzyme plays a role. It allows a more evidence-based approach for animal-to-human extrapolation. Two studies have applied population PKs and physiologically-based PK (PBPK) modeling approaches to analyze quantitative results generated in human-CYP3A4-transgenic mouse models in order to predict human exposure.[20,21] We described the extrapolation of four compounds in human-CYP3A4-transgenic mouse models to humans using a population PK approach. The use of a population PK approach enabled the authors to correct for species differences they assumed to be relevant for the compounds concerned, resulting in more accurate predictions of the human exposure with human-CYP3A4-transgenic compared to wild-type mouse models. Zhang et al. used a PBPK modeling approach in combination with a boosting effect study of ritonavir on NVS123 in a human-CYP3A4-transgenic mouse model. Hereby, not only the human exposure could be accurately predicted, but a DDI involving CYP3A4 was described as well. Choo et al. reported that under specific conditions the transgenic mouse model may be a useful tool to predict the relative contribution of hepatic and intestinal metabolism. They anticipate that in future PBPK modeling in combination with in vitro data will help to clarify the utility and limitations of the transgenic models. To summarize, PK modeling approaches can help to correct for interspecies differences that are expected to contribute to deviations in the predictions. Nevertheless, this requires prior knowledge of interspecies differences (e.g., differences in gastrointestinal tract pH, enzyme

or transporter expression, or binding partners proteins) and therefore FIH dose predictions remain difficult. Human-CYP3A4-transgenic mouse models, extended with modeling approaches, are therefore probably best suited to more accurately predict CYP3A4 inhibition and induction DDIs in a quantitative way, for compounds for which there is already some clinical PK data is available to correct the human-CYP3A4-transgenic mouse models extrapolation to humans and validate predictions.

AUTHOR CONTRIBUTIONS

D.D., A.H.S., J.H.B., A.D.R.H., and T.P.C.D wrote the manuscript. D.D., J.H.B., T.P.C.D., and A.D.R.H. designed the research. D.D. performed the research. D.D. analyzed the data.

FUNDING INFORMATION

No funding was received for this work.

CONFLICT OF INTEREST STATEMENT

The authors declared no competing interests for this work.

DATA AVAILABILITY STATEMENT

The datasets generated during and/or analyzed during the current study are available from the corresponding author on reasonable request.

ORCID

David Damoiseaux https://orcid.org/0000-0002-2348-5923
Jos H. Beijnen https://orcid.org/0000-0003-0118-561X
Thomas P. C. Dorlo https://orcid.org/0000-0003-3076-8435

REFERENCES

1. US Food and Drug Administration. Center for Drug Evaluation and Research, *Guidance for industry estimating the maximum safe starting dose in initial clinical trials for therapeutics in adult healthy volunteers*. 2005.
2. Committee for Medicinal Products for Human Use. European Medicines Agency, *Guideline on strategies to identify and mitigate risks for first-in-human and early clinical trials with investigational medicinal products* – Revision 1. 2017.
3. Committee for Medicinal Products for Human Use. European Medicines Agency, *Guideline on requirements for first-in-man clinical trials for potential high-risk medicinal products*. 2007.
4. International Council for Harmonisation of Technical Requirements for Pharmaceuticals for Human Use. *Safety guideline – S9 nonclinical evaluation for anticancer pharmaceuticals*. 2009.
5. World Health Organisation. *Guidance document for the use of data in development of Chemical-Specific Adjustment Factors (CSAFs) for interspecies differences and human variability in dose/concentration–response assessment*. 2001.
6. Bissig KD, Han W, Barzi M, et al. P450-humanized and human liver chimeric mouse models for studying xenobiotic metabolism and toxicity. *Drug Metab Dispos*. 2018;46(11):1734-1744.
7. van Herwaarden AE, Wagenaar E, van der Kruijssen CMM, et al. Knockout of cytochrome P450 3A yields new mouse models for understanding xenobiotic metabolism. *J Clin Invest*. 2007;117(11):3583-3592.
8. Zanger UM, Schwab M. Cytochrome P450 enzymes in drug metabolism: regulation of gene expression, enzyme activities, and impact of genetic variation. *Pharmacol Ther*. 2013;138(1):103-141.
9. Page MJ, McKenzie JE, Bossuyt PM, et al. The PRISMA 2020 statement: an updated guideline for reporting systematic reviews. *Rev Esp Cardiol (Engl Ed)*. 2021;74(9):790-799.
10. Huwaldt JA. *Plot Digitizer. version 2.6.9*. 2020 https://sourceforge.net/projects/plotdigitizer/files/plotdigitizer/2.6.9/
11. West GB, Brown JH, Enquist BJ. A general model for the origin of allometric scaling laws in biology. *Science*. 1997;276(5309):122-126.
12. White CR, Seymour RS. Mammalian basal metabolic rate is proportional to body mass2/3. *Proc Natl Acad Sci U S A*. 2003;100(7):4046-4049.
13. Abe S, Kobayashi K, Oji A, et al. Modification of single-nucleotide polymorphism in a fully humanized CYP3A mouse by genome editing technology. *Sci Rep*. 2017;7(1):15189.
14. Cheung C, Yu AM, Chen CS, et al. Growth hormone determines sexual dimorphism of hepatic cytochrome P450 3A4 expression in transgenic mice. *J Pharmacol Exp Ther*. 2006;316(3):1328-1334.
15. Hasegawa M, Kapelyukh Y, Tahara H, et al. Quantitative prediction of human pregnane X receptor and cytochrome P450 3A4 mediated drug–drug interaction in a novel multiple humanized mouse line. *Mol Pharmacol*. 2011;80(3):518-528.
16. Kazuki Y, Kobayashi K, Aueviriyavit S, et al. Trans-chromosomic mice containing a human CYP3A cluster for prediction of xenobiotic metabolism in humans. *Hum Mol Genet*. 2013;22(3):578-592.
17. Ma X, Cheung C, Krausz KW, et al. A double transgenic mouse model expressing human pregnane X receptor and cytochrome P450 3A4. *Drug Metab Dispos*. 2008;36(12):2506-2512.
18. Uehara S, Higuchi Y, Yoneda N, et al. An improved TK-NOG mouse as a novel platform for humanized liver that overcomes limitations in both male and female animals. *Drug Metab Pharmacokinet*. 2022;42:100410.
19. Scheer N, Kapelyukh Y, Rode A, et al. Defining human pathways of drug metabolism in vivo through the development of a multiple humanized mouse model. *Drug Metab Dispos*. 2015;43(11):1679-1690.
20. Damoiseaux D, Li W, Martínez-Chávez A, et al. Predictiveness of the human-CYP3A4-transgenic mouse model (Cyp3aXAV) for human drug exposure of CYP3A4-metabolized drugs. *Pharmaceuticals (Basel)*. 2022;15(7):860.
21. Zhang J, Heimbach T, Scheer N, et al. Clinical exposure boost predictions by integrating cytochrome P450 3A4-humanized mouse studies with PBPK modeling. *J Pharm Sci*. 2016;105(4):1398-1404.
22. van Hoppe S, Rood JJM, Buil L, et al. P-glycoprotein (MDR1/ABCB1) restricts brain penetration of the Bruton's tyrosine kinase inhibitor Ibrutinib, while cytochrome P450-3A (CYP3A) limits its Oral bioavailability. *Mol Pharm*. 2018;15(11):5124-5134.

23. Kumar R, Mota LC, Litoff EJ, et al. Compensatory changes in CYP expression in three different toxicology mouse models: CAR-null, Cyp3a-null, and Cyp2b9/10/13-null mice. *PloS One*. 2017;12(3):e0174355.
24. McConnell EL, Basit AW, Murdan S. Measurements of rat and mouse gastrointestinal pH, fluid and lymphoid tissue, and implications for in-vivo experiments. *J Pharm Pharmacol*. 2008;60(1):63-70.
25. Evans DF, Pye G, Bramley R, Clark AG, Dyson TJ, Hardcastle JD. Measurement of gastrointestinal pH profiles in normal ambulant human subjects. *Gut*. 1988;29(8):1035-1041.
26. Crabbe JC, Wahlsten D, Dudek BC. Genetics of mouse behavior: interactions with laboratory environment. *Science*. 1999;284(5420):1670-1672.
27. Karp NA, Speak AO, White JK, et al. Impact of temporal variation on design and analysis of mouse knockout phenotyping studies. *PloS One*. 2014;9(10):e111239.
28. Ubink R, Dirksen EHC, Rouwette M, et al. Unraveling the interaction between carboxylesterase 1c and the antibody-drug conjugate SYD985: improved translational PK/PD by using Ces1c knockout mice. *Mol Cancer Ther*. 2018;17(11):2389-2398.
29. Tang SC, Kort A, Cheung KL, et al. P-glycoprotein, CYP3A, and plasma carboxylesterase determine brain disposition and oral availability of the novel taxane cabazitaxel (Jevtana) in mice. *Mol Pharm*. 2015;12(10):3714-3723.
30. Tang SC, Sparidans RW, Cheung KL, et al. P-glycoprotein, CYP3A, and plasma carboxylesterase determine brain and blood disposition of the mTOR inhibitor everolimus (Afinitor) in mice. *Clin Cancer Res*. 2014;20(12):3133-3145.
31. Granvil CP, Yu AM, Elizondo G, et al. Expression of the human CYP3A4 gene in the small intestine of transgenic mice: in vitro metabolism and pharmacokinetics of midazolam. *Drug Metab Dispos*. 2003;31(5):548-558.
32. van Herwaarden AE, Smit JW, Sparidans RW, et al. Midazolam and cyclosporin a metabolism in transgenic mice with liver-specific expression of human CYP3A4. *Drug Metab Dispos*. 2005;33(7):892-895.
33. Choo EF, Woolsey S, DeMent K, et al. Use of transgenic mouse models to understand the oral disposition and drug-drug interaction potential of cobimetinib, a MEK inhibitor. *Drug Metab Dispos*. 2015;43(6):864-869.
34. Damoiseaux D, Li W, Beijnen JH, Schinkel AH, Huitema ADR, Dorlo TPC. Population pharmacokinetic modelling to support the evaluation of preclinical pharmacokinetic experiments with Lorlatinib. *J Pharm Sci*. 2022;111(2):495-504.
35. Hasegawa M, Tahara H, Inoue R, Kakuni M, Tateno C, Ushiki J. Investigation of drug-drug interactions caused by human pregnane X receptor-mediated induction of CYP3A4 and CYP2C subfamilies in chimeric mice with a humanized liver. *Drug Metab Dispos*. 2012;40(3):474-480.
36. Henderson CJ, Kapelyukh Y, Scheer N, et al. An extensively humanized mouse model to predict pathways of drug disposition and drug/drug interactions, and to facilitate design of clinical trials. *Drug Metab Dispos*. 2019;47(6):601-615.
37. Kim S, Pray D, Zheng M, et al. Quantitative relationship between rifampicin exposure and induction of Cyp3a11 in SXR humanized mice: extrapolation to human CYP3A4 induction potential. *Drug Metab Lett*. 2008;2(3):169-175.
38. Kobayashi K, Kuze J, Abe S, et al. CYP3A4 induction in the liver and intestine of pregnane X receptor/CYP3A-humanized mice: approaches by mass spectrometry imaging and portal blood analysis. *Mol Pharmacol*. 2019;96(5):600-608.
39. Li W, Sparidans RW, Wang Y, et al. P-glycoprotein (MDR1/ABCB1) restricts brain accumulation and cytochrome P450-3A (CYP3A) limits oral availability of the novel ALK/ROS1 inhibitor lorlatinib. *Int J Cancer*. 2018;143(8):2029-2038.
40. Li W, Sparidans RW, Wang Y, Lebre MC, Beijnen JH, Schinkel AH. Oral coadministration of elacridar and ritonavir enhances brain accumulation and oral availability of the novel ALK/ROS1 inhibitor lorlatinib. *Eur J Pharm Biopharm*. 2019;136:120-130.
41. Li W, Sparidans R, el-lari M, et al. P-glycoprotein (ABCB1/MDR1) limits brain accumulation and cytochrome P450-3A (CYP3A) restricts oral availability of the novel FGFR4 inhibitor fisogatinib (BLU-554). *Int J Pharm*. 2020;573:118842.
42. Li W, Tibben M, Wang Y, et al. P-glycoprotein (MDR1/ABCB1) controls brain accumulation and intestinal disposition of the novel TGF-β signaling pathway inhibitor galunisertib. *Int J Cancer*. 2020;146(6):1631-1642.
43. Ly JQ, Messick K, Qin A, Takahashi RH, Choo EF. Utility of CYP3A4 and PXR-CAR-CYP3A4/3A7 transgenic mouse models to assess the magnitude of CYP3A4 mediated drug–drug interactions. *Mol Pharm*. 2017;14(5):1754-1759.
44. MacLeod AK, McLaughlin LA, Henderson CJ, Wolf CR. Activation status of the pregnane X receptor influences vemurafenib availability in humanized mouse models. *Cancer Res*. 2015;75(21):4573-4581.
45. MacLeod AK, Lin D, Huang JT–J, McLaughlin LA, Henderson CJ, Wolf CR. Identification of novel pathways of osimertinib disposition and potential implications for the outcome of lung cancer therapy. *Clin Cancer Res*. 2018;24(9):2138-2147.
46. Martínez-Chávez A, van Hoppe S, Rosing H, et al. P-glycoprotein limits Ribociclib brain exposure and CYP3A4 restricts its Oral bioavailability. *Mol Pharm*. 2019;16(9):3842-3852.
47. Martínez-Chávez A, Loos NHC, Lebre MC, et al. ABCB1 and ABCG2 limit brain penetration and, together with CYP3A4, total plasma exposure of abemaciclib and its active metabolites. *Pharmacol Res*. 2022;178:105954.
48. Miura T, Uehara S, Shimizu M, et al. Different roles of human cytochrome P450 2C9 and 3A enzymes in diclofenac 4′- and 5-hydroxylations mediated by metabolically inactivated human hepatocytes in previously transplanted chimeric mice. *Chem Res Toxicol*. 2020;33(2):634-639.
49. Martins MLF, Loos NHC, Mucuk S, et al. P-glycoprotein (ABCB1/MDR1) controls brain penetration and intestinal disposition of the PARP1/2 inhibitor Niraparib. *Mol Pharm*. 2021;18(12):4371-4384.
50. van Waterschoot RA, Rooswinkel RW, Sparidans RW, et al. Inhibition and stimulation of intestinal and hepatic CYP3A activity: studies in humanized CYP3A4 transgenic mice using triazolam. *Drug Metab Dispos*. 2009;37(12):2305-2313.
51. Wang J, Bruin MAC, Gan C, et al. Brain accumulation of tivozanib is restricted by ABCB1 (P-glycoprotein) and ABCG2 (breast cancer resistance protein) in mice. *Int J Pharm*. 2020;581:119277.
52. Yamazaki H, Suemizu H, Murayama N, et al. In vivo drug interactions of the teratogen thalidomide with midazolam: heterotropic cooperativity of human cytochrome P450 in humanized TK-NOG mice. *Chem Res Toxicol*. 2013;26(3):486-489.
53. Patnaik A, Rosen LS, Tolaney SM, et al. Efficacy and safety of abemaciclib, an inhibitor of CDK4 and CDK6, for patients with breast cancer, non-small cell lung cancer, and other solid tumors. *Cancer Discov*. 2016;6(7):740-753.

54. Friedman H, Redmond DE Jr, Greenblatt DJ. Comparative pharmacokinetics of alprazolam and lorazepam in humans and in African green monkeys. *Psychopharmacology (Berl)*. 1991;104(1):103-105.
55. Abbas R, Hug BA, Leister C, Burns J, Sonnichsen D. Effect of ketoconazole on the pharmacokinetics of oral bosutinib in healthy subjects. *J Clin Pharmacol*. 2011;51(12):1721-1727.
56. Rosen LS, LoRusso P, Ma WW, et al. A first-in-human phase I study to evaluate the MEK1/2 inhibitor, cobimetinib, administered daily in patients with advanced solid tumors. *Invest New Drugs*. 2016;34(5):604-613.
57. Xu H, O'Gorman M, Tan W, Brega N, Bello A. The effects of ketoconazole and rifampin on the single-dose pharmacokinetics of crizotinib in healthy subjects. *Eur J Clin Pharmacol*. 2015;71(12):1441-1449.
58. Gupta SK, Manfro RC, Tomlanovich SJ, Gambertoglio JG, Garovoy MR, Benet LZ. Effect of food on the pharmacokinetics of cyclosporine in healthy subjects following oral and intravenous administration. *J Clin Pharmacol*. 1990;30(7):643-653.
59. Ouellet D, Grossmann KF, Limentani G, et al. Effects of particle size, food, and capsule shell composition on the oral bioavailability of dabrafenib, a BRAF inhibitor, in patients with BRAF mutation-positive tumors. *J Pharm Sci*. 2013;102(9):3100-3109.
60. Christopher LJ, Cui D, Wu C, et al. Metabolism and disposition of dasatinib after oral administration to humans. *Drug Metab Dispos*. 2008;36(7):1357-1364.
61. Leuratti C, Loprete L, Rossini M, Frangione V, Rovati S, Radicioni M. Pharmacokinetics and safety of a diclofenac sodium 75 mg/1 mL solution (Akis(®)/Dicloin(®)) administered as a single intravenous bolus injection in healthy men and women. *Eur J Drug Metab Pharmacokinet*. 2019;44(5):681-689.
62. Baker SD, Sparreboom A, Verweij J. Clinical pharmacokinetics of docetaxel: recent developments. *Clin Pharmacokinet*. 2006;45(3):235-252.
63. Kim RD, Sarker D, Meyer T, et al. First-in-human phase I study of Fisogatinib (BLU-554) validates aberrant FGF19 signaling as a driver event in hepatocellular carcinoma. *Cancer Discov*. 2019;9(12):1696-1707.
64. Ding X, Gueorguieva I, Wesley JA, Burns LJ, Coutant CA. Assessment of in vivo clinical product performance of a weak basic drug by integration of in vitro dissolution tests and physiologically based absorption modeling. *AAPS J*. 2015;17(6):1395-1406.
65. Ranson M, Hammond LA, Ferry D, et al. ZD1839, a selective oral epidermal growth factor receptor-tyrosine kinase inhibitor, is well tolerated and active in patients with solid, malignant tumors: results of a phase I trial. *J Clin Oncol*. 2002;20(9):2240-2250.
66. Tapaninen T, Olkkola AM, Tornio A, et al. Itraconazole increases Ibrutinib exposure 10-fold and reduces interindividual variation-a potentially beneficial drug–drug interaction. *Clin Transl Sci*. 2020;13(2):345-351.
67. Patel M, Chen J, McGrory S, et al. The effect of itraconazole on the pharmacokinetics of lorlatinib: results of a phase I, open-label, crossover study in healthy participants. *Invest New Drugs*. 2019;38:131-139.
68. Stroh M, Dishy V, Radziszewski W, et al. The effects of multiple doses of rolofylline on the single-dose pharmacokinetics of midazolam in healthy subjects. *Am J Ther*. 2010;17(1):53-60.
69. Pentikis HS, Connolly M, Trapnell CB, Forbes WP, Bettenhausen DK. The effect of multiple-dose, oral rifaximin on the pharmacokinetics of intravenous and oral midazolam in healthy volunteers. *Pharmacotherapy*. 2007;27(10):1361-1369.
70. Moore K, Zhang ZY, Agarwal S, Burris H, Patel MR, Kansra V. The effect of food on the pharmacokinetics of niraparib, a poly(ADP-ribose) polymerase (PARP) inhibitor, in patients with recurrent ovarian cancer. *Cancer Chemother Pharmacol*. 2018;81(3):497-503.
71. Ochoa D, Román M, Cabaleiro T, Saiz-Rodríguez M, Mejía G, Abad-Santos F. Effect of food on the pharmacokinetics of omeprazole, pantoprazole and rabeprazole. *BMC Pharmacol Toxicol*. 2020;21(1):54.
72. Planchard D, Brown KH, Kim DW, et al. Osimertinib Western and Asian clinical pharmacokinetics in patients and healthy volunteers: implications for formulation, dose, and dosing frequency in pivotal clinical studies. *Cancer Chemother Pharmacol*. 2016;77(4):767-776.
73. Zhang Q, Wang Z, Wu J, Zhou Z, Zhou R, Hu W. Bioequivalence and pharmacokinetic evaluation of two Oral formulations of Regorafenib: an open-label, randomised, single-dose, two-period, two-way crossover clinical trial in healthy Chinese volunteers under fasting and fed conditions. *Drug des Devel Ther*. 2021;15:3277-3288.
74. Ji Y, Abdelhady AM, Samant TS, Yang S, Rodriguez Lorenc K. Evaluation of absolute Oral bioavailability and bioequivalence of Ribociclib, a cyclin-dependent kinase 4/6 inhibitor, in healthy subjects. *Clin Pharmacol Drug Dev*. 2020;9(7):855-866.
75. Lathia C, Lettieri J, Cihon F, Gallentine M, Radtke M, Sundaresan P. Lack of effect of ketoconazole-mediated CYP3A inhibition on sorafenib clinical pharmacokinetics. *Cancer Chemother Pharmacol*. 2006;57(5):685-692.
76. Cotreau MM, Siebers NM, Miller J, Strahs AL, Slichenmyer W. Effects of ketoconazole or rifampin on the pharmacokinetics of tivozanib hydrochloride, a vascular endothelial growth factor receptor tyrosine kinase inhibitor. *Clin Pharmacol Drug Dev*. 2015;4(2):137-142.
77. Robin DW, Lee MH, Hasan SS, Wood AJJ. Triazolam in cirrhosis: pharmacokinetics and pharmacodynamics. *Clin Pharmacol Ther*. 1993;54(6):630-637.
78. Martin P, Oliver S, Kennedy SJ, et al. Pharmacokinetics of vandetanib: three phase I studies in healthy subjects. *Clin Ther*. 2012;34(1):221-237.
79. Ribas A, Zhang W, Chang I, et al. The effects of a high-fat meal on single-dose vemurafenib pharmacokinetics. *J Clin Pharmacol*. 2014;54(4):368-374.

SUPPORTING INFORMATION

Additional supporting information can be found online in the Supporting Information section at the end of this article.

How to cite this article: Damoiseaux D, Schinkel AH, Beijnen JH, Huitema ADR, Dorlo TPC. Predictability of human exposure by human-CYP3A4-transgenic mouse models: A meta-analysis. *Clin Transl Sci*. 2024;17:e13668. doi:10.1111/cts.13668